WARSAW UNIVERSITY OF TECHNOLOGY Index 351733
FACULTY OF CIVIL ENGINEERING
COMMITTEE FOR CIVIL AND WATER ENGINEERING
POLISH ACADEMY OF SCIENCES ISSN 1230-2945

DOI: 10.24425/ace.2023.144189

ARCHIVES OF CIVIL ENGINEERING

Vol. LXIX ISSUE 1 2023

pp. 571 –591

Research paper

Study on shear performance of cold-formed thin-walled steel-paper straw board composite wall with openings

Xiuhua Zhang[1], Shuijing Xu[2], Siyu Li[3]

Abstract: To explore the application of cold-formed thin-walled steel-paper straw board(CTSPSB) composite wall in practical engineering and further meet people's living requirements, it was proposed to open holes in the composite wall to simulate the doors and windows in practical applications. Two composite wall specimens were tested to study the shear performance of the CTSPSB composite wall. Through the analysis of specimens' damage forms and experimental data, the characteristic values of bearing capacity and lateral stiffness were obtained. And then, the model of the composite wall was built by ANSYS, and finite element analysis (FEA) results were consistent with the experimental results, which could verify the feasibility of the finite element model. Moreover, the model needed to open holes and extensive parameter analysis was carried out. The FEA results indicate the most reasonable distance between screws around the opening is 150 mm; the most suitable spacing between the small studs is 400 mm; the position of the opening has the least influence on the shear performance, and the difference between the results of the five groups of models is within 5%; while the width of the opening has the greatest impact on the shear performance. Compared with the wall without opening, the bearing capacity of the wall with an opening width of 600 mm, 1200 mm and 1800 mm decreases by 38%, 46% and 52% respectively. Besides, the calculation formula of shear capacity of CTSPSB composite wall with openings was improved, which could be used as experience for practical engineering.

Keywords: cold-formed thin-walled steel, composite structures, finite element methods, paper straw board, shear performance

[1]Prof., DSc., PhD., Eng., Dept. of Civil Engineering, Northeast Forestry University, Harbin 150040, China, e-mail: zhangxh2000@163.com, ORCID: 0000-0001-9565-1081
[2]MSc., Eng., Dept. of Civil Engineering, Northeast Forestry University, Harbin 150040, China, e-mail: 3477936653@qq.com, ORCID: 0000-0002-7659-6862
[3]MSc., Eng., Dept. of Civil Engineering, Northeast Forestry University, Harbin 150040, China, e-mail: 1175674943@qq.com, ORCID: 0000-0003-2482-4330

1. Introduction

Cold-formed thin-walled steel (CTS) composite wall [1] is made of steel as the keel, with gypsum board, plywood or thin steel plates as sheathing boards, which is connected together by self-tapping screws. And the wall has the advantages of lightweight and high strength, easy construction and recyclability.

In recent years, a large number of research had been conducted on the structural properties of CTS composite wall, such as its tensile-compressive properties [2–4], bending resistance [5], seismic performance [6, 7], progressive collapse [8], fire resistance [9], shear performance [10–13], surface characteristics and mechanical property changes after corrosion [14], and distribution of residual stresses [15]. Through these researches and analyses, it could be concluded that the damage to the composite wall was inseparable from its shear performance. Baran [16] studied the shear performance of the CTS composite wall, and the results showed that the damage to the CTS composite wall was mainly manifested in the local buckling damage to the studs in the compression zone; Zhou Xuhong et al. [17] studied the shear performance of CTS residential composite wall by analyzing the factors influencing the shear performance of composite wall and concluded that the vertical load, the cross-sectional dimensions of the wall frame studs and the stud spacing could affect the shear performance of the composite wall. Wang Chungang [18] did an experimental study on the shear performance of CTS composite walls reinforced by corner braces and concluded that for steel frame walls, the set of corner braces made the load no longer concentrated at the diagonal brace nodes, prevented the cross brace from deforming significantly and its screw shearing at the connection, and increased the bearing capacity and displacement ductility coefficient by about 40% and 17%, respectively.

Nowadays, the traditional CTS composite wall could no longer meet the building requirements, so people began to seek and invent a new type of composite wall. Chen Zhihua [19] proposed a CTS shear wall of built-in straw board, welded to mesh cement mortar protection layer, and found that the wall still had significant horizontal load bearing capacity even with severe cracking. Ahmed Sheta [20] wrapped around CTS with polyethylene-carbon fiber cloth to give them a much higher load capacity. Zhang's team [21–23] combined CTS with a straw board which was wrapped with protective paper to form a new composite wall, that is CTSPSB composite wall, and then conducted a lot of experiments and FEA on it to obtain mechanical properties, this creative point also provided a lot of inspiration.

And this year, the Chinese government [24] also set a carbon emission reduction target, with CO_2 emissions peaking before 2030, striving to achieve carbon neutrality by 2060. Since the construction industry accounted for 42% of Chinese greenhouse gas emissions [25], the construction industry could make a significant contribution to the reduction of greenhouse gas emissions. Therefore, research on the application of CTSPSB composite walls is necessary.

In this paper, based on the horizontal monotonic loading experiment of two CTSPSB composite walls of the literature [23], the model of the composite wall was built by ANSYS.

In order to simulate the doors and windows, the models needed to be open holes, and then extensive parameters were studied to obtain the influence on the CTSPSB composite wall with openings. Through analysis, the influence laws of different factors on the failure mode and ultimate load of the composite wall were obtained, and the shear capacity calculation formula of the CTSPSB composite wall with openings was improved, which provided references for the practical engineering of the CTSPSB composite wall with openings in the future.

2. Experimental process and data analysis

2.1. Experimental specimens

In the literature [23], two CTSPSB composite wall specimens were designed for the loading experiments. The construction of the composite wall was displayed in Fig. 1.

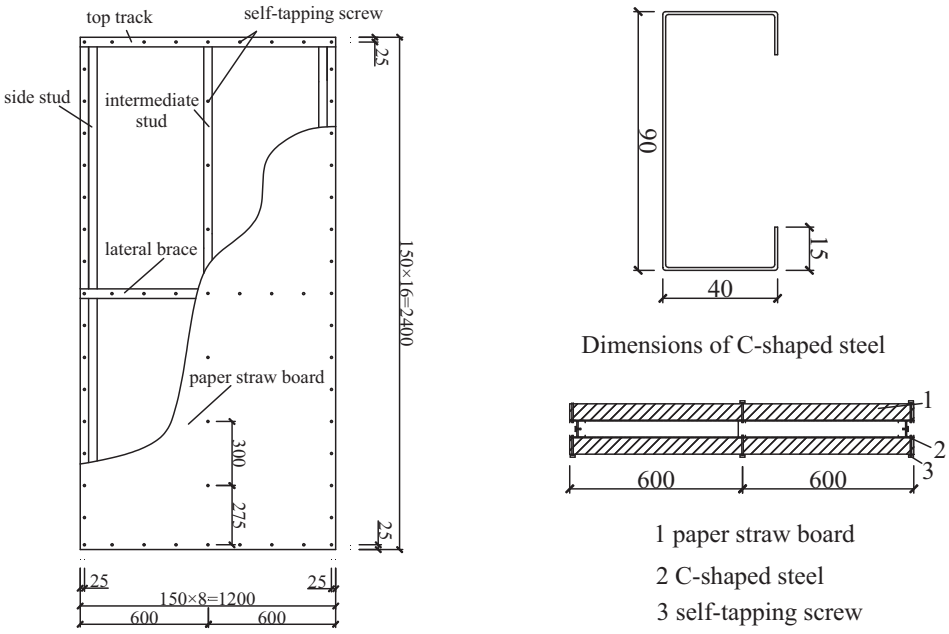

(a) The structural form (b) The section form

Fig. 1. The structural form and section form of the CTSPSB composite wall

The size of the PSB was 2400 mm × 1200 mm × 58 mm (height × width × thick); the three studs of the wall steel frame were designed as C90 mm×40 mm×15 mm×1 mm; the size of section steel for the top track and bottom track both were U93 mm×45 mm×1.5 mm; the lateral brace also adopted in U-shaped steel, with the size of U93 mm×45 mm×1 mm;

and steel frame covered with PSB on both sides. In addition, the spacing between the screws used between the PSB and the side stud was 150 mm, the spacing between the screws used between the PSB and the intermediate stud was 300 mm; as well as spacing between the screws used between the PSB and the top track and bottom track was 150 mm. The parameters of the CTSPSB composite wall were displayed in Table 1.

Table 1. CTSPSB composite wall parameters

Specimen No.	Specimen size ($L \times H$) /mm	Steel keel form	Sheathing board form	Vertical load /kN
W-DAS-1	1200×2400	Cross brace	Double-sided	0
W-DAS-2	1200×2400	Cross brace	Double-sided	15

The PSB takes straw as raw material. During the production process, the straw without binder is placed in an airtight container to form a dense board by heating and extruding. After the board is shaped, it is wrapped with a protective paper coated with binder on one side. The PSB has the characteristics of good heat insulation and sound insulation performance, low thermal conductivity, anti-combustion, waterproof and pest prevention. Moreover, according to the experimental results [23], the various material parameters are displayed in Table 2.

Table 2. The material parameters of CTSPSB composite wall

Material	Elastic Modulus /MPa	Poisson's ratio	Yield Strength /MPa	Tangent modulus /MPa
1.5 mm thick steel	1.98×10^5	0.3	274.3	1.98×10^3
1.0 mm thick steel	1.97×10^5	0.3	255.82	1.97×10^3
PSB	400.6	0.336	1.87	

2.2. Experimental process

The first step of the method of adding load was to add 2 kN each time and kept it for about 2 minutes and recorded the load-displacement curves of the specimens in real-time. When there was a significant change in the slope of the curves, it was changed to displacement-controlled adding load. And then the load and displacement data onto the specimens were collected by the computer until the specimens were not suitable to continue loading or the load dropped to 85% of the peak value of the load-displacement curve.

2.3. Experimental phenomena

The experimental phenomena of the specimen was displayed in Fig. 2.

(a) (b) (c) (d)

Fig. 2. The experimental phenomena of specimen: (a) Cracking of PSB, (b) Bending of side stud, (c) Depression of the screw, (d) Overall deformation of the wall

2.4. Analysis of experimental results

2.4.1. Analysis of load-displacement curves

Through the observation and recording of the experimental data, the load-displacement curves of the two CTSPSB composite wall specimens were displayed in Fig. 3. It could be seen from Fig. 3 that with the increase of vertical load on the upper part of the CTSPSB composite wall, the slope of the load-displacement curves also increased in the first(elasticity stage) and second (yield stage) stages, indicating that increasing the vertical load of the CTSPSB composite wall could enhance the interaction between the section steel frame and the two sides of the PSB, which could improve the overall stability of the wall.

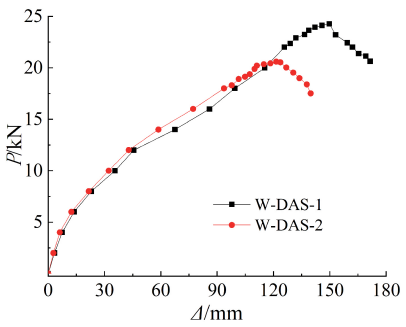

Fig. 3. Load-displacement curves of the two specimens

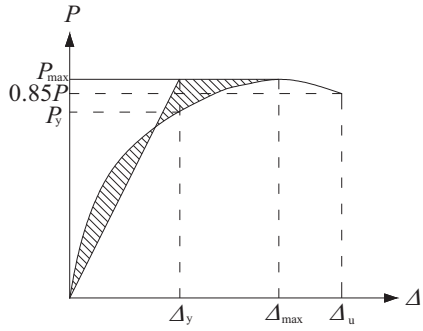

Fig. 4. The method of energy equivalent area

2.4.2. The ductility coefficient and lateral stiffness

This paper, mainly uses the load-displacement curves to calculate the yield load and limit load. The bearing capacity characteristic values of the composite walls were calculated according to the America Standard [26]. The calculation method used the method of energy equivalent area (Fig. 4) to determine the yield load P_y, yield displacement Δ_u, the limit load corresponded to 0.85 times the maximum load value, and the ductility coefficient was calculated as Δ_u/Δ_y.

Through analysis and calculation of the experimental results, the parameters related to the shear performance of the specimens were displayed in Table 3.

Table 3. Parameters related to the shear performance of CTSPSB composite wall specimens

Specimen No.	Yield point		Peak point		Limit point		Ductility coefficient	Lateral stiffness
	P_y kN	Δ_y mm	$P_{\max}$ kN	$\Delta_{\max}$ mm	P_u kN	Δ_u mm	μ	K kN/m
W-DAS-1	20.13	115.27	24.28	149.75	20.64	171.54	1.49	348
W-DAS-2	16.81	83.90	20.60	121.54	17.51	139.82	1.67	370

3. Finite element method analysis

3.1. Establishment of finite element model

3.1.1. Element selection

The steel frame used in this paper contained cold-formed thin-walled C-section steel and U-section steel. The galvanized CTS was Q235 and its thickness was 1 mm and 1.5 mm respectively, therefore, shell element SHELL181 was used to simulate the cold-formed thin-walled C and U sections. The PSB had a height of 2400 mm and a thickness of 58 mm. According to the division rule of the plate and shell structure, it satisfied $(5\div8) < L/h < (80\div100)$, which could be regarded as a thin board. Therefore, the PSB also adopted SHELL181.

By combining the experimental phenomena, it could be seen that was no slipping deformation between the internal components of the steel frame, and the self-tapping screws only played a connecting role, so the coupling method could be directly used to deal with it. However, the screws connecting the steel frame and PSB were inclined, and the slip deformation between the two materials was very serious so the amount of slip between the two materials could not be ignored. Therefore, the element COMBIN39 was used to simulate the self-tapping screw. The simulation of the screws was displayed in Fig. 5.

During the loading process of the composite wall, the sliding amount of the spring element was mainly controlled by the squeeze deformation amount of the wall with openings

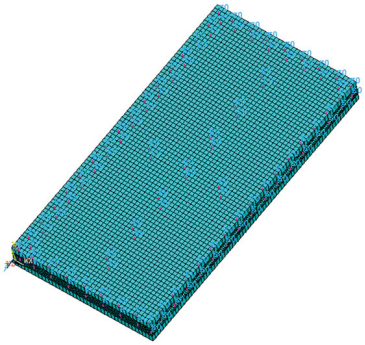

Fig. 5. Simulation of screws

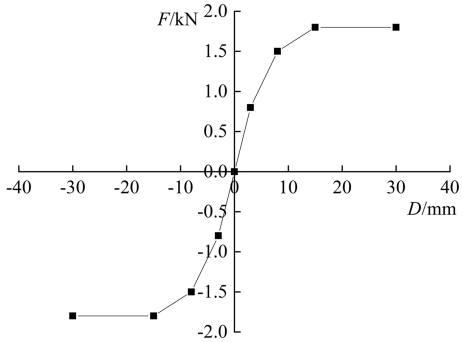

Fig. 6. Spring stiffness curve

on the sheathing board, and the spring stiffness was a discrete and large value. According to the experimental data [23], the shear force of the self-tapping screw is 3.14 kN, and the spring stiffness curve (Fig. 6) was used to simulate the self-tapping screw.

3.1.2. Constitutive relationship of materials

Before building the model, the constitutive relationship of the materials should be known. In order to obtain more accurate FEA results, this paper adopted the nonlinear analysis for FEA. In the process of modeling, the Huber-Von Mises yield criterion and follow-up criterion were adopted. To better fit the experimental data of the composite wall, the material parameters were based on the material property experimental data of the PSB and steel (Fig. 7). The material parameters of steel and PSB were shown in section 2.1.

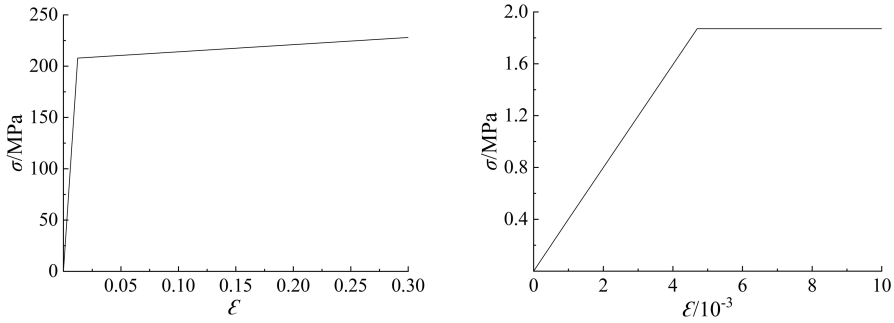

(a) Steel (b) PSB

Fig. 7. Constitutive relationship of materials

3.1.3. Establishment and meshing of finite element models

This paper adopted the bottom-up modeling method to create key points in turn, line, surface, and finally form a geometric model. The model adopted the mapped meshing method, the mesh size of the steel frame was 15 mm × 15 mm, and the PSB was

30 mm × 30 mm, which could ensure that the mesh division was relatively uniform and obtained ideal results. When meshing, selected each surface, in turn, to mesh it separately. The modeling process of the composite wall was displayed in Fig. 8.

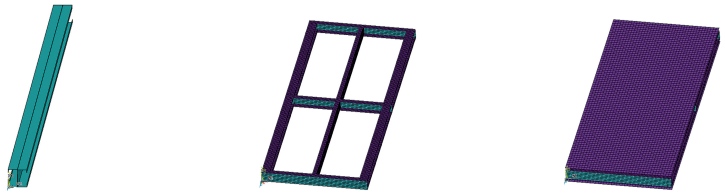

(a) Side column (b) Complete steel frame model (c) Composite wall meshing

Fig. 8. Composite wall modeling process

3.2. Validation of finite element model

The experimental specimens W-DAS-1 and W-DAS-2 were horizontally monotonically loaded, and the load-displacement curves obtained in FEA were compared with the load-displacement curves obtained in the experiment, as displayed in Fig. 9. The yield load obtained from the FEA of specimen W-DAS-1 was 3.2% higher than the experimental yield load, and the maximum bearing capacity was 3.3% higher than the experimental maximum bearing capacity; the yield load obtained from the FEA of specimen W-DAS-2 was 3.0% higher than the experimental yield load, and the maximum bearing capacity was 7.0% higher than the experimental maximum bearing capacity. It could be seen that in the initial stage of loading, the load-displacement curve of the finite element model and the experimental wall was in good agreement. With the continuous increase of displacement, there was a large difference between the limit displacement. This is because in the finite element analysis, considering that the sett of various conditions of the model was in an

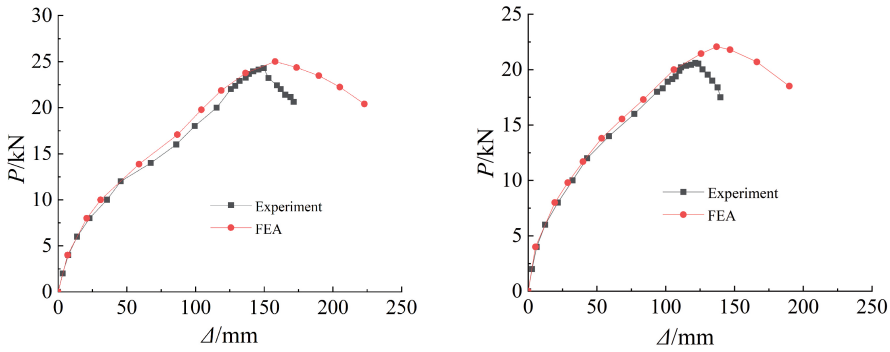

(a) W-DAS-1 (b) W-DAS-2

Fig. 9. Comparison of load-displacement curves between experiment and FEA

ideal state, while in the actual experiment operation, the wall assembly steps were complex, and there were certain errors in the manual assembly of the wall. Therefore, the ultimate displacement of the model obtained in the later stage of the FEA had a large deviation from the ultimate displacement of the experimental wall, but during the loading process, the curve showed that the two trends were similar, and the error was controlled within 10%, which verified the feasibility of the FEA method used in this paper.

By comparing the damage modes of specimens W-DAS-1 and W-DAS-2 in the FEA and experiment, it was found that the two were in good agreement. The main damage characteristics were as follows:

When the finite element model of specimen W-DAS-1 was under load, the damage phenomenon was similar to the experimental phenomenon, both of which were local buckling of the side bottom stud under pressure, meanwhile, the wall surface self-tapping screws were depressed in many places, and the integrity of the PSB on both sides was good. With the increase of displacement, local buckling first occurred on the side bottom studs, and the flanges on both sides of the lateral braces were bent slightly. The comparison of damage modes was displayed in Fig. 10 and Fig. 11.

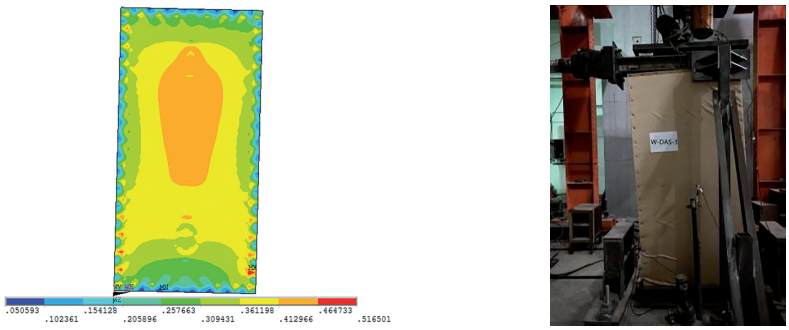

(a) FEA (b) Experiment

Fig. 10. Comparison of the overall damage mode for specimen W-DAS-1

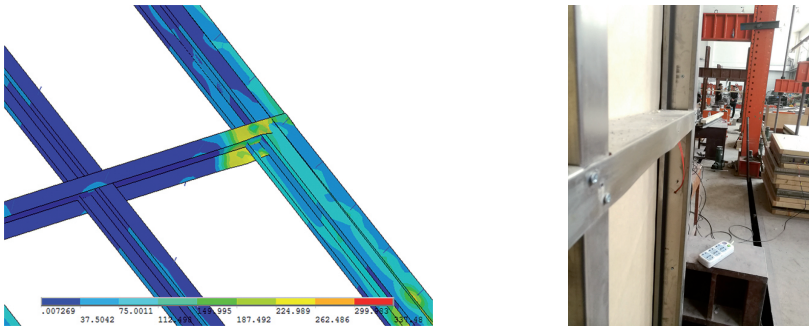

(a) FEA (b) Experiment

Fig. 11. Comparison of the damage mode of lateral brace for specimen W-DAS-2

3.3. FEA of CTSPSB composite wall with openings

In real application, the wall always opens holes to meet the needs of daily life. In order to study the influence of the opening on the CTSPSB composite wall, the finite element models of the composite walls with openings were designed. Analyzing the influence of different wall widths, screw spacing, opening position, opening rate, etc on the shear capacity of the walls. The finite element simulation parameters were displayed in Table 4.

Table 4. Parameter design of the CTSPSB composite walls with openings

Specimen Model No.	Opening size (Width × height) mm	Opening rate %	Opening area m^2
DQ1224-1-L	600 × 300	6.25%	0.18
DQ1224-2-L	600 × 600	12.5%	0.36
DQ1224-3-L	600 × 1200	25%	0.72
W2424-0	0 × 0	0	0
DQ2424-1-L	600 × 600	6.25%	0.36
DQ2424-2-M	600 × 1200	12.50%	0.72
DQ2424-3-M	1200 × 600	12.50%	0.72
DQ2424-4-T	1200 × 600	12.50%	0.72
DQ2424-5-B	1200 × 600	12.50%	0.72
DQ2424-6-R	1200 × 600	12.50%	0.72
DQ2424-7-L	1200 × 600	12.50%	0.72
DQ2424-8-M	1200 × 1200	25%	1.44
DQ2424-9-M	1200 × 1200	25%	1.44
DQ2424-10-M	1200 × 1200	25%	1.44
DQ2424-11-R	1800 × 1200	37.50%	2.16

Note: W means wall; DQ means the wall with openings; 1224 represents a composite wall with a width of 1200 0mm and a height of 2400 mm; the numbers –1, –2, etc. represent the numbers of the walls with different openings; the symbols of –L, –R represents the position of the opening relative to the wall.

3.3.1. The influence of screw spacing

Considering that the opening is a weak force-bearing area of the structure, relevant structural measures should be strengthened. In the set of the screw spacing, if the screw spacing is too sparse, it will not have a good fixing effect; if the screw spacing is too close, there will be a larger work during installation. Generally, the screw spacing of 300 mm, 150 mm, and 100 mm is adopted, so this section discusses the impact of the three kinds of screw spacing on the bearing capacity of the wall. Based on the experimental model

DQ1224-2-L (Fig. 12), the spacing of the screw around the opening between the PSB and steel frame is changed to 150 mm and 100 mm respectively to play a strengthening role. Other construction methods and parameter settings are the same as the composite wall without opening. The specific data is displayed in Fig. 13.

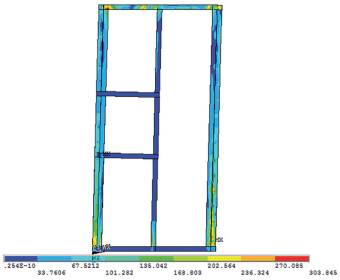

Fig. 12. The steel frame of DQ1224-2-L

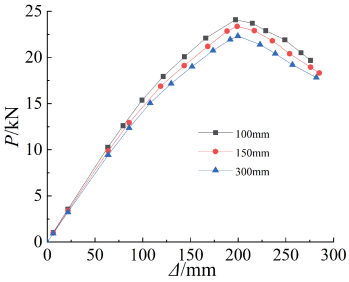

Fig. 13. Comparison of load-displacement curves

Through the analysis, the maximum bearing capacity of the wall at screw spacing of 300 mm is only 23.01 kN, while the wall at screw spacing of 150 mm is 23.84 kN and the wall at screw spacing of 100 mm is 24.09 kN. The maximum bearing capacity is increased by 3.6% and 4.69% respectively by reducing the screw spacing from 300 mm to 150 mm and 100 mm. Therefore, the reduction of screw spacing in a certain range can effectively improve the shear performance of the wall, the following models of CTSPSB composite walls with openings at the screw spacing all are designed as 150 mm.

3.3.2. The influence of the opening rate

To explore the influence of the opening rate on the CTSPSB composite wall with openings, there are two cases. The first case is a wall with the same dimensions and different opening rates. For model DQ2424-8-M, the opening height is increased by 200 mm on the basis of model DQ2424-3-M, and other constructive measures and FEA methods remain unchanged. The stress cloud diagram of the model DQ2424-8-M after the solution is displayed in Fig. 14. It can be seen from the cloud diagram that the wall is evenly inclined under horizontal load, and the top of the wall has the largest displacement; the most severe part of the steel frame damage occurs at the bottom of the side stud; the stud at the opening is not equipped with reinforcement measures, and the four corners of the PSB at the opening are seriously destroyed.

The load-displacement curves of models W2424-0, DQ2424-3-M, and DQ2424-8-M are shown in Fig. 15. The curves show that the shear capacity of walls with openings is significantly lower than that of walls without opening, and the width of the opening of all the three models is 1200 mm, only the height of the opening increases from 600 mm to 1200 mm, and the bearing capacity is reduced by 13.05%.

The second case is to keep the opening rate constant, the wall size is not the same. For example, the opening rates of models DQ1224-1-L and DQ2424-1-L are both 6.25%; DQ1224-2-L and DQ2424-7-L are both 12.50%; DQ1224-3-L and DQ2424-8-M are

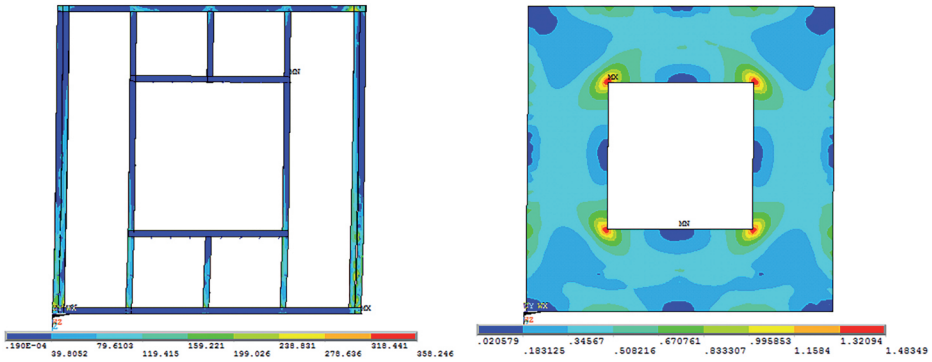

(a) Steel frame (b) PSB

Fig. 14. The stress cloud diagram of DQ2424-8-M

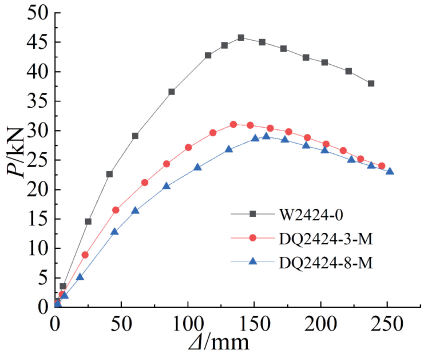

Fig. 15. Comparison of the analysis results

both 25%. By performing FEA on these three groups of walls, the results show that the damage mode of the wall has little relationship with its size when the opening rate is the same, and the maximum shear loads of the walls are similar when the size of the walls is the same. The load-displacement curves are drawn as displayed in Fig. 16.

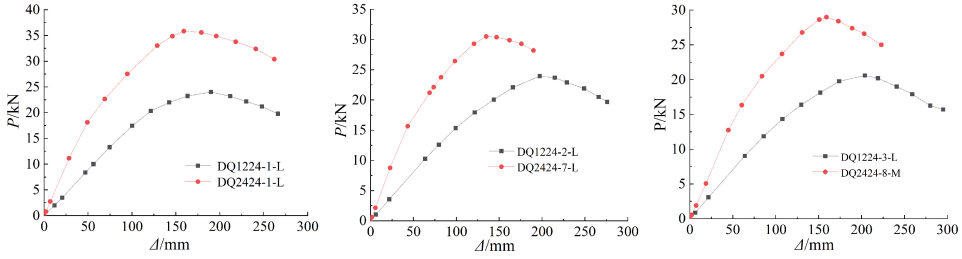

(a) The opening rate is 6.25% (b) The opening rate is 12.5% (c) The opening rate is 25%

Fig. 16. Comparison of the analysis results of the opening rate in the second case

It can be seen from the analysis of the two cases, the results show that the CTSPSB composite wall with openings lacks part of the PSB, which weakens the effect of the skin diaphragm. With the increase of the opening area, the supporting capacity provided by the PSB for the steel frame is also reduced. And the existence of the opening has a certain weakening effect on the shear capacity of the overall wall, but it has a certain degree of improvement on the ductility of the wall. At the same time, the PSB will be relatively deformed along with the steel frame, which can show composite wall has a certain ductility performance. Since the constraint of the model is set at the bottom of the model and the horizontal force is applied at the top of the model, the overall horizontal translation phenomenon appears at the top of the opening, and the horizontal displacement of the composite wall gradually decreases from top to bottom, thus showing the characteristics of shear deformation.

3.3.3. The influence of opening width

To study the influence of opening width on the shear capacity of the CTSPSB composite wall, the opening width of model DQ2424-11-R (Fig. 17) is designed to be 1800 mm, which is compared with model DQ2424-2-M (Fig. 18) with an opening width of 600 mm and

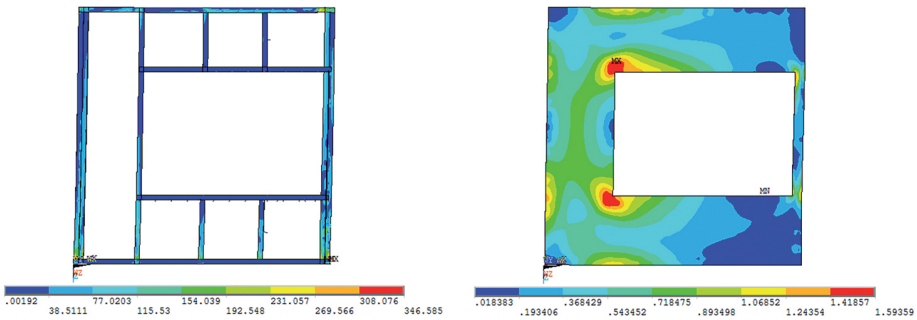

(a) Steel frame (b) PSB

Fig. 17. The stress cloud diagram of DQ2424-11-R

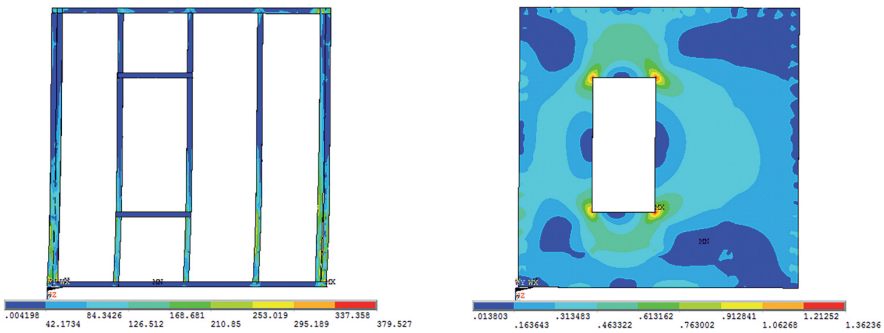

(a) Steel frame (b) PSB

Fig. 18. The stress cloud diagram of DQ2424-2-M

model DQ2424-8-M (Fig. 14) with an opening width of 1200 mm respectively. From the stress cloud diagram, as the opening width increases, the deformation of the steel frame on the bottom side also increases and the stress concentration phenomenon of the PSB becomes more obvious.

According to the simulation data, the load-displacement curves are plotted in Fig. 19. The results show that the greater the width of the opening, the more significant drop in shear capacity. The maximum load of the other three walls is reduced by 38%, 46% and 52% respectively compared to the wall without opening (model W2424-0). The reason for the analysis result may be that the increase in the width of the opening involves the removal of more section steel studs and the reduction of sheathing board, resulting in a significant reduction in shear capacity.

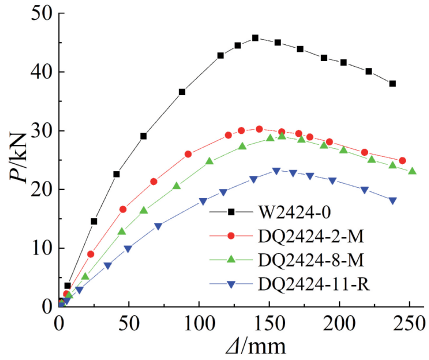

Fig. 19. Comparison of different opening widths

3.3.4. The influence of the opening position

This section is mainly adopted in the wall (2400 mm × 2400 mm) with the same size opening (1200 mm × 600 mm), only changing the opening position, and to study the influence of the change of opening position on the shear capacity of the wall. For this purpose, two control groups are set up, namely, the first case is that the height of the opening remains the same, and only the horizontal position is changed; the second case is that the horizontal position of the opening remains the same, and only the height of the opening is changed.

(1) On the basis of model DQ2424-3-M (Fig. 20), the position of the opening is set near the right stud side to get model DQ2424-6-R (Fig. 21); set near the left stud side to get model DQ2424-7-L (Fig. 22), other constructive measures and analysis methods remain unchanged.

Comparing models DQ2424-6-R and DQ2424-7-L stress cloud diagram after the solution, it can be seen that when the position of the opening is close to the left or right studs, the PSB is mainly damaged by tearing in the middle two corners; while model DQ2424-3-M shows that the four corners of the board are slightly damaged, and the rest of the board is more evenly stressed. From this, it can be considered that the PSB plays a supporting role in the compression area, and the side stud strengthening measures can

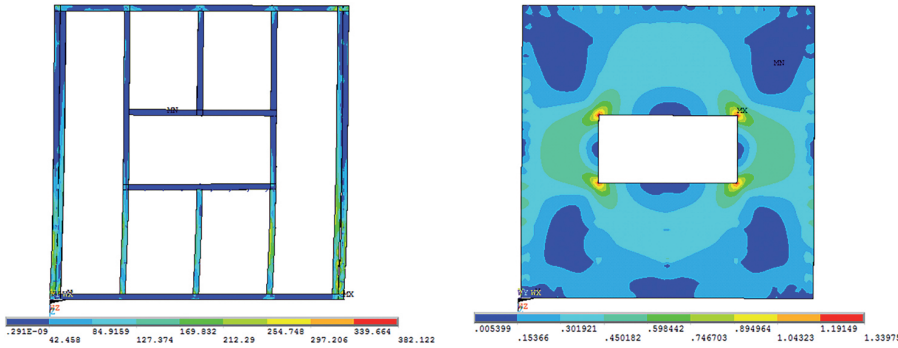

(a) Steel frame (b) PSB

Fig. 20. The stress cloud diagram of DQ2424-3-M

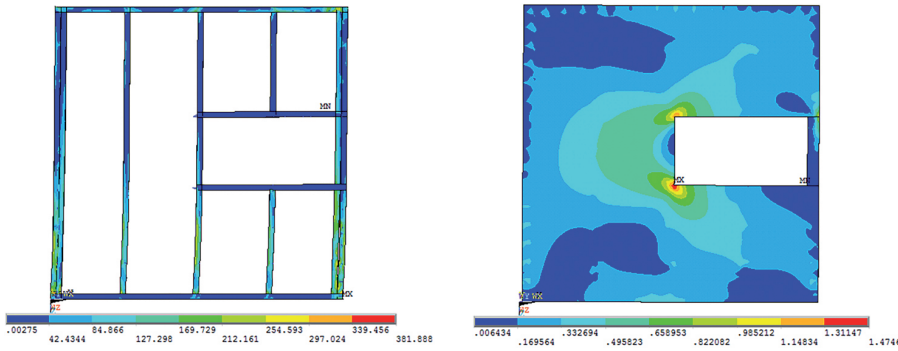

(a) Steel frame (b) PSB

Fig. 21. The stress cloud diagram of DQ2424-6-R

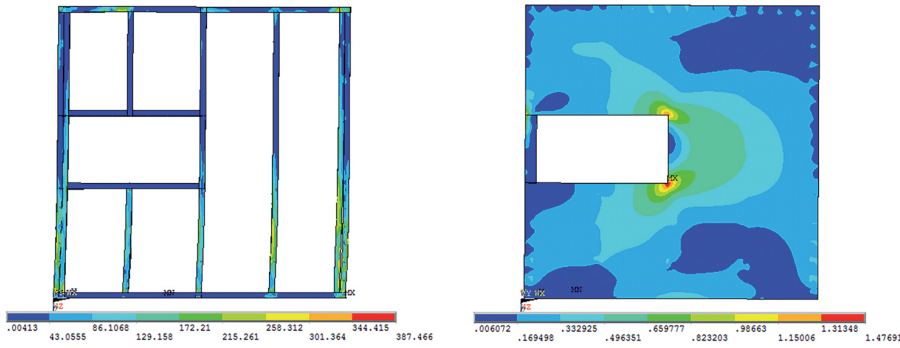

(a) Steel frame (b) PSB

Fig. 22. The stress cloud diagram of DQ2424-7-L

also avoid damage to the four corner parts of the PSB opening. The load-displacement curves of the three models are displayed in Fig. 23. The curves show that the three lines are almost overlapped, the image trends are very similar, and the maximum bearing capacity is not much different.

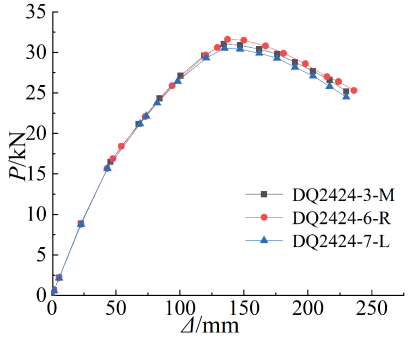

Fig. 23. The load-displacement curves in the first case

(2) For the purpose of studying the influence of the different positions of top, middle and bottom on shear capacity, the models DQ2424-4-T (Fig. 24) and DQ2424-5-B (Fig. 25) are designed to make a comparison with model DQ2424-3-M. It can be found from the stress cloud diagram that when the opening is located near the top, the stress concentration at the corners of the opening is more serious than when the opening is set at the bottom, so it can be concluded that the stress concentration can be better avoided by sett the opening at the middle and bottom side of the wall. The curves (Fig. 26) show that the maximum load of model DQ2424-5-B is slightly higher than that of model DQ2424-4-T and model DQ2424-3-M. Generally speaking, the difference between the results of the five groups of models is within 5%, the opening position has almost no influence on the shear capacity of the wall.

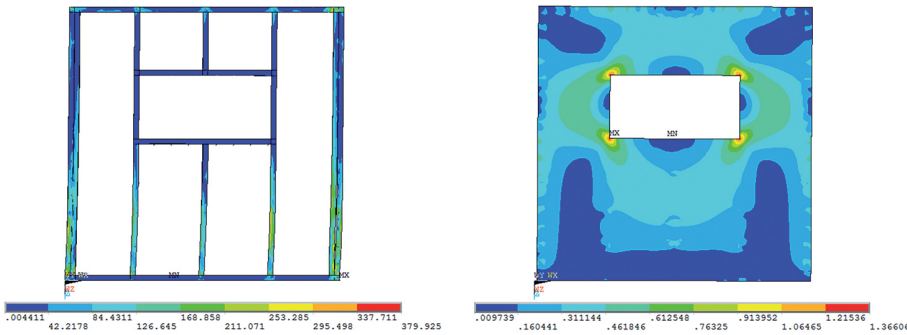

(a) Steel frame (b) PSB

Fig. 24. The stress cloud diagram of DQ2424-4-T

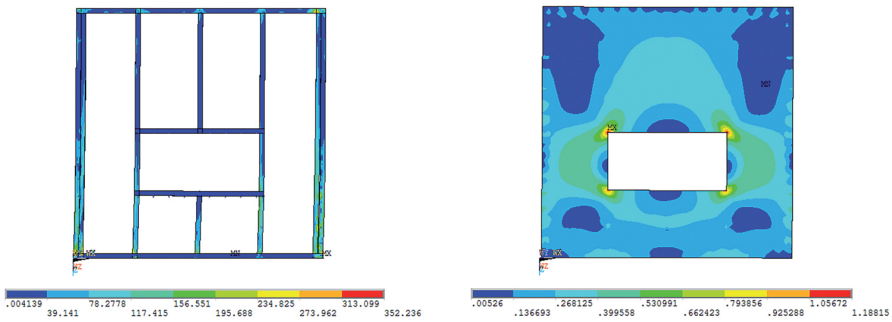

(a) Steel frame (b) PSB

Fig. 25. The stress cloud diagram of DQ2424-5-B

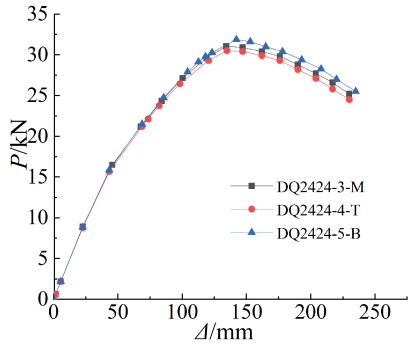

Fig. 26. The load-displacement curve in the second case

3.3.5. The influence of short studs above and below the opening

When the width of the opening increases to a certain degree, the sett of short studs above and below can play a role in reinforcement. In order to study its change rule, the models (Fig. 27) DQ2424-9-M and DQ2424-10-M, corresponding to the spacing of small short studs of 300 mm and 400 mm, respectively, add different numbers of small short studs on the basis of model DQ2424-8-M to analyze the change of its shear capacity.

And the analysis results are displayed in Fig. 28. Comparing the curves, the three curves are not much different at the initial stage; when the maximum load is reached in the middle and late stages, the curves show a big difference. The maximum bearing capacity of model DQ2424-9-M with two short studs and model DQ2424-10-M with three short studs are 31.72 kN and 32.98 kN respectively, which are increased by 10.49% and 13.8% respectively compared to model DQ2424-8-M with only one short stud.

Therefore, it can be seen that: appropriately increasing the small studs can effectively improve the shear performance of the wall, while too many small studs are uneconomical, and too few have no obvious effect. Through analysis, the spacing between the small studs is more suitable to be 400mm, which not only controls a certain economic efficiency but also plays a good effect in enhancing the shear performance of the wall.

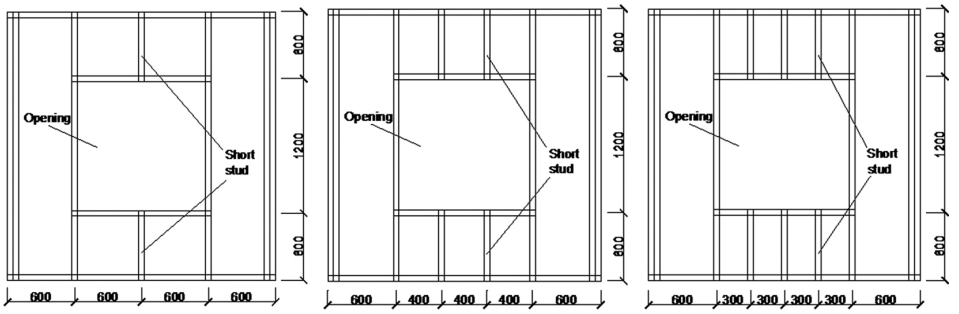

(a) DQ2424-8-M (b) DQ2424-9-M (c) DQ2424-10-M

Fig. 27. The steel frame dimensions of the three models

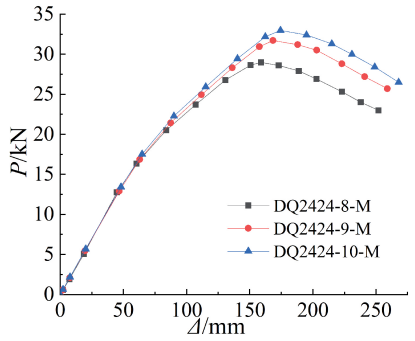

Fig. 28. Analysis results of different small short studs

4. Calculation of shear capacity

The discussion on the calculation formula of the shear capacity of the composite wall with openings has always been a hot topic all around the world. Some scholars [27, 28] have conducted relevant research and analysis. According to existing data, the formula for shear bearing capacity of the CTSPSB composite wall with openings has been improved, as follows:

$$P' = \alpha P \tag{4.1}$$

$$\alpha = \frac{\gamma}{3 - 2\gamma} \tag{4.2}$$

$$\gamma = \frac{1}{1 + \frac{A_0}{H \sum L_i}} \tag{4.3}$$

where: P' is the shear capacity of the composite wall with openings; P is the shear capacity of the composite wall without opening; α is the shear capacity reduction factor; γ is the ratio of opening to the entire wall; A_0 is the total area of the opening; H is the height of the wall; $\sum L_i$ is the total length of wall components without opening.

Based on the previous finite element parameter analysis, as well as the relevant data and load-displacement curves obtained, the change in the position of the opening is not significant in terms of the overall impact on the overall wall shear capacity; and the opening rate and the width of the opening is the factor that makes the shear capacity of the wall change in a relatively large magnitude. Therefore, in this paper, when discussing the calculation method for the composite wall with opening, the opening position is not taken into account, only considering the influence of the opening rate. Through the comparison of the maximum load, it can be seen the results calculated by the formula are very close to those of FEA.

The results obtained by the FEA method and the formula method are drawn into broken lines for comparison and analysis, as displayed in Fig. 29.

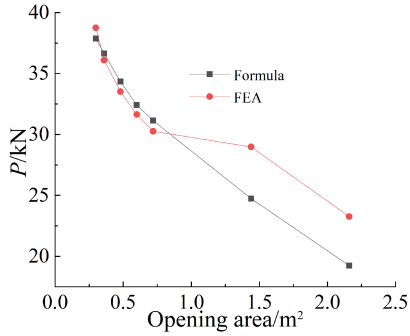

Fig. 29. Comparison of results of different calculation methods

When the opening rate does not exceed 25%, the ratio of the FEA result and the formula method calculation result is very close; when the opening rate increases by more than 25%, the error is relatively large. This is because the formula calculation method takes into account the need to provide more safety reserves for large opening, and the calculation result of the formula used is smaller than that of the finite element method. It shows that the calculation model used in this paper is reasonable and the calculation method used is feasible, thus verifying that the formula is suitable.

5. Conclusions

1. The FEA results are consistent with the experimental phenomena, and the main damage mode of the CTSPSB composite wall with openings is the local buckling failure at the bottom of the CTS side stud. Due to the good integrity of the PSB, the PSB on both sides provides a good constraint on the steel frame to improve the overall strength of the wall.
2. Different screw spacing, different opening rates, different spacing of small short studs and different opening widths have a great impact on the wall. Among them, the influence of opening width is the most obvious. Compared with the composite wall without opening, the maximum bearing capacity of the wall with opening width

of 1800 mm is reduced by 52%, the reason is that the increase in opening width involves the removal of more steel studs.

3. The appropriate reduction of the screw spacing of the sheathing board at the opening is beneficial to the improvement of the shear capacity of the wall with, and the screws are less costly as well as easy to install. After the FEA in this paper, it is suggested that in the actual engineering, the screw spacing at the opening is set to 150 mm, which makes the connection of the screws at the opening part play a certain strengthening role.
4. The four corners of the sheathing board at the opening are areas where the force is weaker. Some measures should be taken to encrypt the screw spacing at right angles to improve the force performance of the wall.
5. Through data analysis and theoretical derivation, the shear capacity calculation formula of the CTSPSB composite wall with openings was improved. And the FEA result and the formula method calculation result are very close when the opening rate does not exceed 25%.

Acknowledgements

This research is financially supported by the National Natural Science Foundation of China (51878130).

References

[1] X.H. Zhou, Y. Shi, et al., "Low-rise cold-formed thin-walled steel residential system", *Journal of Building Science and Engineering*, vol. 22, no. 2, pp. 1–14, 2005 (in Chinese).

[2] M. Peiris and M. Mahendran, "Behaviour of cold-formed steel lipped channel sections subject to eccentric axial compression", *Journal of Constructional Steel Research*, vol. 184, art. no. 106808, 2021, DOI: 10.1016/j.jcsr.2021.106808.

[3] L.C.M. Vieira, Y. Shifferaw, and B.W. Schafer, "Experiments on Sheathed Cold-formed Steel Studs in Compression", *Journal of Constructional Steel Research*, vol. 67, no. 10, pp. 1554–1566, 2011, DOI: 10.1016/j.jcsr.2011.03.029.

[4] Y. Dias, M. Mahendran, et al., "Axial compression strength of gypsum plasterboard and steel sheathed web-stiffened stud walls", *Thin-Walled Structures*, vol. 134, pp. 203–219, 2019, DOI: 10.1016/j.tws.2018.10.013.

[5] W.T. Qiao, X.S. Yan, R.J. Zhu, F.Y. Wang, and D. Wang, "Flexural properties of new cold-formed thin-walled steel and concrete composite slabs", *Journal of Building Engineering*, vol. 31, art. no. 101441, 2020, DOI: 10.1016/j.jobe.2020.101441.

[6] R.Q. Feng, et al., "Seismic performance of cold-formed steel framed shear walls with steel sheathing and gypsum board", *Thin-Walled Structures*, vol. 143, art. no. 106238, 2019, DOI: 10.1016/j.tws.2019.106238.

[7] I. Shamim, J. DaBreo, et al., "Dynamic testing of single-and double-story steel-sheathed cold-formed steel-framed shear walls", *Journal of Structural Engineering*, vol. 139, no. 5, pp. 807–817, 2013, DOI: 10.1061/(ASCE)ST.1943-541X.0000594.

[8] W.Y. Zeng, J. Luo, et al., "Resistance to Progressive collapse performance analysis of steel open-web sandwich plate structure", *Archives of Civil Engineering*, vol. 66, no. 3, pp. 281–303, 2020, DOI: 10.24425/ace.2020.134398.

[9] P. Samiee, et al., "Fire performance of cold-formed steel shear wall with different steel grade and thicknesses", *Structures*, vol. 29, pp. 751–770, 2021, DOI: 10.1016/j.istruc.2020.11.073.

[10] N.L. Rahim, et al., "Effect of bolt configurations on stiffness for steel-wood-steel connection loaded parallel to grain for softwoods in Malaysia", *Archives of Civil Engineering*, vol. 68, no. 3, pp. 323–338, 2022, DOI: 10.24425/ace.2022.141888.

[11] Y.X. Zou, X.H. Zhou, et al., "Shear resistance of cold-formed thin-walled steel inter-story connections", *Journal of Constructional Steel Research*, vol. 183, art. no. 106757, 2021, DOI: 10.1016/j.jcsr.2021.106757.

[12] Y.P. Chu, X.R. He, Y. Yao, and H.J. Hou, "Experimental Research on the Shear Performance of the Two-Storey Composite Cold-Formed Thin-Walled Steel Wall", *KSCE Journal of Civil Engineering*, vol. 24, no. 2, pp. 537–550, 2019, DOI: 10.1007/s12205-020-0519-y.

[13] K. Falkowicz, "Experimental and numerical analysis of compression thin-walled composite plates weakened by cut-outs", *Archives of Civil Engineering*, vol. 63, no. 4, pp. 161–172, 2017, DOI: 10.1515/ace-2017-0047.

[14] B. Nie, S.H. Xu, et al., "Surface morphology characteristics and mechanical properties of corroded cold-formed steel channel sections", *Journal of Building Engineering*, vol. 42, art. no. 102786, 2021, DOI: 10.1016/j.jobe.2021.102786.

[15] M. Ayad, N. Yidris, et al., "An investigation on longitudinal residual strains distribution of thin-walled press-braked cold formed steel sections using 3D FEM technique", *Heliyon*, vol. 4, no. 11, pp. 1–17, 2018, DOI: 10.1016/j.heliyon.2018.e00937.

[16] E. Baran and C. Alica, "Behavior of Cold-formed Steel Wall Panels under Monotonic Horizontal Loading", *Journal of Constructional Steel Research*, vol. 79, no. 7, pp. 1–18, 2012, DOI: 10.1016/j.jcsr.2012.07.020.

[17] X.H. Zhou, Y. Shi, et al, "Research on the shear performance of cold-formed thin-walled steel residential composite walls", *Journal of Building Structures,* vol. 27, no. 3, pp. 42–47, 2006, DOI: 10.14006/j.jzjgxb.2006.03.006 (in Chinese).

[18] C.G. Wang, Y.D. Li, et al., "Experimental study on the shear performance of corner braced reinforced cold-formed thin-walled steel composite walls", *Journal of Building Structures*, vol. 41, no. S2, pp. 291–303, 2020, DOI: 10.14006/j.jzjgxb.2020.S2.0032 (in Chinese).

[19] Z.H. Chen, et al., "Experimental study on seismic behavior of cold-formed steel shear walls with reinforced plastered straw-bale sheathing", *Thin-Walled Structures*, vol. 169, art. no. 108303, 2021, DOI: 10.1016/j.tws.2021.108303.

[20] A. Sheta, et al., "Structural performance of novel thin-walled composite cold-formed steel/PE-ECC beams", *Thin-Walled Structures*, vol. 162, art. no. 107586, 2021, DOI: 10.1016/j.tws.2021.107586.

[21] X.H. Zhang, E.Y. Zhang, et al., "Study on shear performance of cold-formed thin-walled steel walls sheathed by paper straw board, *Engineering Structures*, vol. 245, art. no. 112873, 2021, DOI: 10.1016/j.engstruct.2021.112873.

[22] A. Shen, X.H. Zhang, et al., "Study on shear performance of cold-formed thin-walled steel straw board composite wall", *Forest Products Industry*, vol. 58, no. 07, pp. 32–39, 2021, DOI: 10.19531/j.issn1001-5299.202107007 (in Chinese).

[23] J.C. Yang, "Experimental study on the shear resistance of cold-formed thin-walled C-section steel-strawboard composite walls", M.A. thesis, Northeast Forestry University, China, 2018 (in Chinese).

[24] M. Li, "China will formulate an action plan for peaking carbon emissions by 2030". [Online]. Available: http://www.gov.cn/zhengce/2021-03/06/content_5590830.htm. [Accessed: 6 Mar. 2021] (in Chinese).

[25] Y. Jiang, S. Hu, Y. Zhang, *Annual Development Research Report on China Building Energy Efficiency*. Beijing, China: China Architecture and Building Press, 2021 (in Chinese).

[26] ASTM E2126-07 Standard test methods for cyclic (Reversed) load test for shear resistance of walls for buildings. American National Standards Institute, 2007.

[27] H. Darvishi and M. Mofid, "Structural performance assessment of large unstiffened openings in steel plate shear walls", *Engineering Structures*, vol. 247, art. no. 112966, 2021, DOI: 10.1016/j.engstruct.2021.112966.

[28] M. Vatandoust, M. Riyazi, A. Joshaghani, and M. Balapour, "Optimization of Coupled Shear Walls Openings Dimensions under Static Loading using Continuous Method", *KSCE Journal of Civil Engineering*, vol. 22, no. 12, pp. 5074–5083, 2018, DOI: 10.1007/s12205-017-1608-4.

Received: 2022-09-13, Revised: 2022-11-29